This is the Author's Accepted Manuscript version of the paper:
Y. Weng, R. Salehi, X. Ge, D. Rizzo, M. P. Castanier, S. Heim, and T. Ersal, "Model-Free Speed Management for a Heterogeneous Platoon of Connected Ground Vehicles," Journal of Intelligent Transportation Systems: Technology, Planning, and Operations, doi:10.1080/15472450.2020.1797506, 2020.

Model-Free Speed Management for a Heterogeneous Platoon of Connected Ground Vehicles

Yifan Weng[a], Rasoul Salehi[a] , Xinyi Ge[a], Denise Rizzo[b], Matthew P. Castanier[b], Scott Heim[b] and Tulga Ersal[a]

[a]Department of Mechanical Engineering, University of Michigan, Ann Arbor, MI 48109, USA.
[b]U.S. Army Ground Vehicle Systems Center, Warren, MI 48092, USA.

ARTICLE HISTORY
Compiled August 8, 2020

ABSTRACT
Motivated by military applications, this work considers connected platoons of ground vehicles of potentially different sizes and presents a model-free approach for optimizing the speed of the platoon to adjust the trade-off between fuel economy and mobility as measured by travel speed. The motivation to seek a model-free solution is twofold: (1) vehicle models that are typically assumed to be available in model-based methods are not available on-board for military vehicles; (2) a model-free solution can offer robustness to modeling errors. Therefore, in this paper, the problem of optimizing the trade-off between fuel economy and mobility of a mixed platoon is formulated as an optimization problem and solved using the model-free Nelder-Mead approach. To explore the performance characteristics of this approach, a case study is performed with two different size vehicles that are representative of military trucks, both in simulation and in a novel networked engine-in-the-loop setup. The results show that the proposed approach can achieve the desired balance between fuel economy and mobility in a model-free manner despite the nonlinearity caused by gear shift deadzones, albeit at the expense of relatively slow convergence time. In addition, a design guideline for the parameters in the Nelder-Mead approach is also discussed.

KEYWORDS
Model-free Optimization, Platoon, Fuel Economy, Connected Vehicles

1. Introduction

Fuel supply is a critical need and a safety concern for the operation of the large U.S. army vehicular fleet. In a battlefield, up to 80% of logistics comprise large size fuel supply trucks, which are hard to protect (Hargreaves, 2011). An energy-efficient fleet would reduce refueling needs and the risk of a war zone operation, thereby saving lives (Aliotta, 2017).

Several possible solutions to achieve better fuel economy are established for single vehicles such as lightweighting, electrification kits, advanced combat engines, single common powertrain lubricants and fuel efficient gear oil (Aliotta, 2017; Hoffenson, Arepally, & Papalambros, 2014). On the other hand, with platooning technology, the whole vehicular convoy including supply trucks and combat vehicles can be managed to achieve better fuel economy and safety.

Platooning refers to a mode of transportation, in which two or more vehicles form a convoy to closely follow each other for the purposes of increased safety, increased utilization of infrastructure, or reduced aerodynamic drag (U.S. Department of Energy, 2019; Varaiya, 1993). Several major projects throughout the world illustrate the benefits of vehicle platooning, such as German truck platooning project KONVOI (Deutschle et al., 2010), the European platooning project SARTRE (Chan, 2012), the California traffic automation program PATH (Chang et al., 1993; Rajamani, Tan, Law, & Zhang, 2000; Zabat, Stabile, Farascaroli, & Browand, 1995),

CONTACT Tulga Ersal. Email: tersal@umich.edu

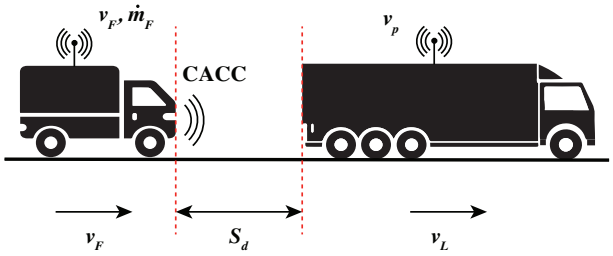

Figure 1.: The heterogeneous platoon with cooperative adaptive cruise control

the grand cooperative driving challenge GCDC (Englund et al., 2016), the Swedish SCANIA platooning project (Bergenhem et al., 2012), and the Japanese truck platooning project Energy ITS (Tsugawa & Kato, 2010; Tsugawa, Kato, & Aoki, 2011).

One important research question in platooning is how to manage a platoon and maximize its benefits, especially in terms of fuel economy and travel time, if the connected vehicle technology is leveraged. To that end, different strategies have been investigated to increase fuel economy during all stages involved in the platooning, including forming/splitting stage and cruising stage. Regarding the former stage, researchers have developed, for example, a coordination algorithm to form platoons of several vehicles from neighboring vehicles and increase fuel saving via reducing the air drag loss (Liang, Mårtensson, & Johansson, 2016). As for the cruising stage, one of the main strategies is the smart management of the speed profile. For example, Caltagirone, Torabi, and Wahde (2015) have used a stochastic optimization procedure to optimize the lead vehicle's speed profile, which can compensate the disturbance caused by terrain change and achieve higher fuel efficiency. Nemeth, Csikos, Varga, and Gaspar (2012) have used the H_∞ control method to solve a multi-criteria optimization problem to find a balance between emission, fuel economy, as well as traveling time criteria. Alam, Mårtensson, and Johansson (2013) have discussed a cooperative control strategy in a heterogeneous platoon based on preview information, which can achieve fuel saving in both uphill and downhill segments. Turri, Besselink, and Johansson (2017) have introduced a framework to generate a fuel-optimal speed profile over different slopes and correspondingly control the vehicle in a real-time manner. Researchers have also proposed the use of a periodic switching control method to reduce the overall fuel consumption of the vehicles in the platoon through a dual-pulse-and-glide operation (Li et al., 2016). Strategies besides smart management of speed have also been considered. For instance, Turri, Besselink, and Johansson (2016) have demonstrated a strategy to select the optimal gear that takes the platoon fuel efficiency into account.

All of the above-mentioned works rely on vehicle models to improve the fuel economy of the platoon. While such vehicle models may be ubiquitous in modern commercial vehicles, they are not readily available on military vehicles, which can hinder the application of model-based techniques to military platoons. Moreover, modeling errors may raise concerns about robustness. Hence, model-free platoon management techniques is of interest for military applications. A model-free approach can also serve as a benchmark for future studies on the value of information available from models, additional measurements or communications for smart management of platoons. However, it is still an open research question to investigate how and to what extent the fuel economy of a platoon of connected vehicles can be improved using model-free methods.

This paper aims to fill this gap by developing and testing a model-free approach to manage a platoon of connected vehicles and optimize the trade-off between fuel economy and mobility of the platoon, where mobility is quantified by the platoon travel speed. In particular, a utility function is formulated that simultaneously considers the fuel economy and speed of the platoon and it is optimized using the Nelder-Mead approach to achieve a model-free solution (Nelder & Mead, 1965). This framework relies on the communication of only instantaneous speed and fuel economy measurements between the vehicles in the platoon and can natively handle platoons of mixed vehicle types. To test the framework, a platoon of two vehicles is considered as illustrated in Figure 1, where a medium duty truck is following a heavy duty truck. Simulations and

networked engine-in-the-loop experiments are utilized to study the effectiveness of the algorithm. Thus, the first original contribution of this paper is the development and simulation based and engine-in-the-loop experimental evaluation of a novel model-free strategy to determine the cruising speed of a connected platoon that can optimally balance the fuel economy and travel speed. In addition, as the second contribution of this paper, a detailed discussion is presented on the nonlinearities of the platoon fuel economy curve, which affect the utility function and the optimization solution in experiments. It is discussed how the hysteresis and discontinuities due to the gear shift logic increases the possibility of converging to a local extremum point. These nonlinearities are neglected in previous works, for example, by assuming a smooth relationship between fuel consumption and vehicle speed (Liang et al., 2016; Nemeth et al., 2012) or ignoring the hysteresis (Caltagirone et al., 2015). Recommendations are made for selecting the tuning parameters in the Nelder-Mead optimization algorithm to mitigate the adverse effect of these nonlinearities on the final optimal solution.

The rest of this paper is organized as follows. In Section 2, an optimal control problem is defined to optimize the fuel economy and travel speed of the platoon. The section also introduces the way the platoon is formed and how the connectivity between the vehicles is established. In Section 3, the models used in the bi-vehicular case study are introduced, including the communication architecture, the vehicular dynamics models and corresponding powertrain models. These models are only needed for the simulation and engine-in-the-loop based evaluations of the developed strategy. The strategy itself, however, is data driven and model free. In Section 4, the optimal control problem is solved using the Nelder-Mead method and results from the simulation study are reported. In Section 5, the sensitivity to the Nelder-Mead parameters is analyzed. Section 6 focuses on the the engine-in-the-loop experiments and describes the networked integration of two engine test cells corresponding to the two vehicle types considered for the case study, as well as the experimental results obtained with this setup. Finally, conclusions are drawn in Section 7 along with a discussion of future research directions.

2. Model-Free Platoon Speed Management

Fuel economy and mobility are the two important considerations for the long-haul military trucks with combustion engine powertrains considered in this study. These two factors are typically in competition with each other. Fuel economy of the platoon $\mathrm{MPG_p}$ is calculated as the harmonic mean of the fuel economy values MPG_i reported by all the N vehicles in the platoon, where

$$\mathrm{MPG}_i := v_\mathrm{p}/\dot{m}_{\mathrm{f},i} \tag{1}$$

is the fuel economy of the ith vehicle ($i = 1, 2, ..., N$) at the cruising speed of v_p with the fuel consumption rate of $\dot{m}_{\mathrm{f},i}$. The use of the harmonic mean is in accordance with the Corporate Average Fuel Economy (CAFE) standard (National Highway Traffic Safety Administration, 2006). Fuel economy can be increased by decreasing the cruising speed of a vehicle and the aerodynamic losses while operating the engine at or near its most efficient operating point, whereas mobility can be improved by increasing the speed. Hence, the simultaneous consideration of these two factors brings about a trade-off, the balancing of which becomes more challenging if multiple mixed-type vehicles are considered simultaneously with different engine characteristics. To address this challenge, the problem is formulated as an optimization problem in this section and solved using the model-free Nelder-Mead method for a convoy of vehicles traveling together at the same speed.

In order to achieve a balance between fuel economy as measured in miles per gallon (MPG)

Table 1.: Parameters of the formulation

Parameter	**Explanation**	**Value**
α_{F}	Weights for fuel economy in (2)	1 MPG^{-1}
α_{M}	Weights for mobility in (2)	0.004 mph^{-2}
$v_{\mathrm{p,des}}$	Desired traveling speed in (2)	60 mph
$v_{\mathrm{p,max}}$	Maximum traveling speed in (3)	70 mph
$v_{\mathrm{p,min}}$	Minimum traveling speed in (3)	10 mph
Γ	Parameter for reflection in Figure 2	0.8
γ	Parameter for expansion in Figure 2	1.5
ρ	Parameter for contraction in Figure 2	0.5
σ	Parameter for shrink in Figure 2	0.5

and mobility M_{p} as measured in travel speed, a utility function J for the platoon is defined as

$$\begin{aligned} J &:= \alpha_{\mathrm{F}}\mathrm{MPG}_{\mathrm{p}} + \alpha_{\mathrm{M}} M_{\mathrm{p}} \\ &:= \alpha_{\mathrm{F}} \frac{N}{\sum_{n=1}^{N} \frac{1}{\mathrm{MPG}_i}} + \alpha_{\mathrm{M}}(v_{\mathrm{p,des}}^2 - (v_{\mathrm{p,des}} - v_{\mathrm{p}})^2). \end{aligned} \tag{2}$$

In (2), $v_{\mathrm{p,des}}$ is the desired speed for the platoon that is assumed to be given based on vehicle and road conditions and determined independent of any fuel economy concerns. The parameters α_{F} and α_{M} are introduced as weights that one selects based on their preference between fuel economy and mobility in a given mission. The higher α_{M} is relative to α_{F}, the more mobility is emphasized and v_{p} approaches $v_{\mathrm{p,des}}$.

The platoon speed v_{p} is calculated by a centralized optimization algorithm in a server assumed to be on-board the lead vehicle. Specifically, the optimal final speed for the platoon v_{p} is calculated by solving the following optimization problem.

$$\begin{aligned} &\max_{v_{\mathrm{p}}} \ J(v_{\mathrm{p}}) \\ &\text{subject to } \ v_{\mathrm{p}} \in [v_{\mathrm{p,min}}, v_{\mathrm{p,max}}] \end{aligned} \tag{3}$$

To solve the optimization problem (3) in a model-free manner, the Nelder-Mead search method is employed as a gradient-free heuristic optimization algorithm. A gradient-free strategy is preferred in this case over a gradient-based one due to the fact that the cost function may not be continuous due to gear shifts and thus gradients may not be always defined.

The flowchart shown in Figure 2 describes the major steps of the Nelder-Mead method as used in this work. In this method, a simplex is formed with vertices that represent a set search points. To seek the best design point, the simplex is transformed iteratively. These transformations can create a mirror image of the current simplex about the side across the worst vertex in the current iteration (reflection), stretch the simplex (expansion), compress it (contraction) or scale it down (shrink). The mathematical expressions for these transformations are shown in Figure 2 and the details can be found in (Nelder & Mead, 1965).

The speed constraints $[v_{\mathrm{p,min}}, v_{\mathrm{p,max}}]$ and the weights α_{M}, α_{F} along with the Nelder-Mead tuning parameters are considered as a set of parameters that can be tuned according to practical requirements such as an acceptable overshoot and convergence time. These parameters are listed in Table 1. The impact of these parameters on the algorithm's performance is discussed more in detail in Section 5.

Note that this heuristic search algorithm allows the optimization to be performed directly with the instantaneous fuel economy data from the vehicles as they travel. However, the fuel

consumption during acceleration or deceleration to v_{p} is different than the fuel required for cruising at $v_{\mathrm{p,des}}$ because of the vehicle inertia. Therefore, the fuel economy measurements need to be made after the platoon settles at the current v_{p} before the next iteration of v_{p} can be calculated by the optimization. This, in turn, will cause a slower convergence than model-based methods. The platoon speed v_{p} is considered to be converged if the speed difference between two successive optimization iterations is smaller than a threshold. In this work, this threshold is set as $\Delta v_{\mathrm{th}} = 0.5$ mph.

The optimization algorithm calculates and transmits v_{p} to all vehicles in the platoon through a vehicle-to-vehicle communication network using Dedicated Short Range Communication (DSRC). Each vehicle is assumed to be equipped with a speed controller that can take v_{p} as a speed setpoint. In particular, a proportional-integral (PI) cruise controller is implemented for the lead vehicle, whereas a connected adaptive cruise control (CACC) architecture is realized for the following vehicles to track v_{p} while maintaining a desired distance S_{d} (see Figure 1) and string stability (Ploeg, Scheepers, van Nunen, van de Wouw, & Nijmeijer, 2011). A brief review of CACC including its architecture, the control method applied and its applications is available in (Z. Wang, Wu, & Barth, 2018). String stability is discussed in various works for heterogeneous vehicle platoons (C. Wang & Nijmeijer, 2015). Zheng, Bian, Li, and Li (2019) have studied the behavior of a heterogeneous vehicle platoon under directed acyclic interactions. Milanés and Shladover (2016) have studied the cut-in response in a string of CACC vehicles. On the other hand, Z. Wang, Wu, Hao, Boriboonsomsin, and Barth (2017) have discussed the possible improvement in energy saving and pollutant emission reduction by proposing an ECO-CACC system. Liu, Shladover, Lu, and Kan (2020) have discussed the potential improvement in the fuel efficiency on highway using CACC.

The CACC considered in this work is illustrated for the special case of a platoon of two vehicles in Figure 3. Each vehicle has an internal PI cruise controller to track the given speed setpoints $v_{\mathrm{L,set}}$ and $v_{\mathrm{F,set}}$ for the lead and the follower vehicles, respectively. The lead vehicle speed setpoint $v_{\mathrm{L,set}}$ is calculated by the platoon optimizer as v_{p}, whereas the follower desired speed is calculated in the Laplace domain as

$$V_{\mathrm{F,set}}(s) = V_{\mathrm{L,set}}(s) + K(s)X_e(s), \tag{4}$$

where $K(s) = c_1 s + c_2$ is a proportional-derivative (PD) controller and

$$X_e(s) = X_L(s) - P(s)X_F(s) \tag{5}$$

is the vehicles' distance tracking error. The transfer function $P(s)$ is called the following policy, which realizes holding a time gap t_g between the two vehicles according to

$$P(s) = t_g s + 1. \tag{6}$$

Therefore,

$$X_{\mathrm{e}}(s) = X_{\mathrm{L}}(s) - X_{\mathrm{F}}(s) - V_{\mathrm{F}}(s)t_g, \tag{7}$$

which means the distance between the two vehicles is calculated based on a selected time gap and the following vehicle speed v_F.

3. Vehicle models for validation

The platoon management framework described in Section 2 is model free. However, to evaluate the framework in simulation and in engine-the-loop experiments, vehicle models are needed to represent the actual vehicles. This section describes the vehicle models used in this work.

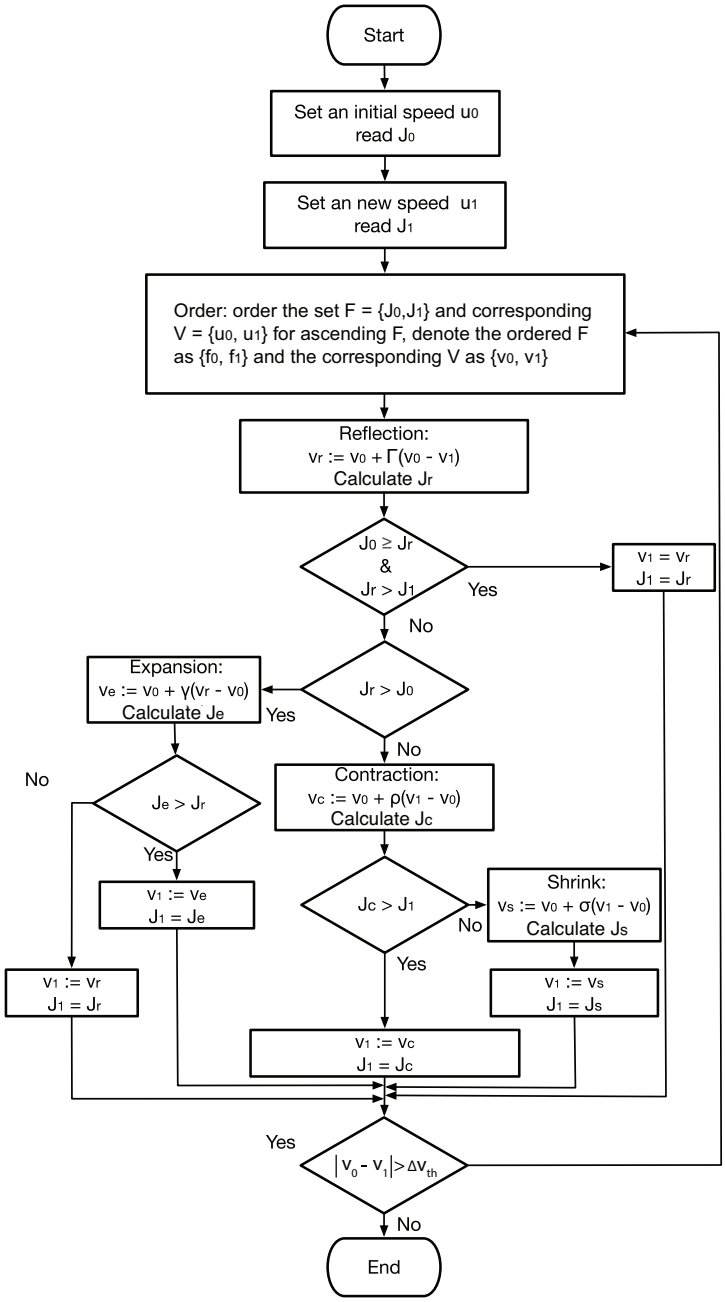

Figure 2.: Flowchart of Nelder-Mead algorithm

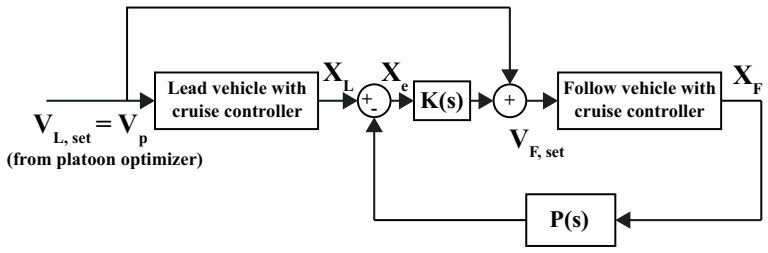

Figure 3.: The CACC architecture realized for a platoon of two vehicles.

In the two-vehicle platoon studied in this work, the lead vehicle is selected as a notional heavy duty vehicle similar to a military heavy tactical vehicle and is assumed to be followed by a notional medium duty vehicle, again similar to a military medium duty truck. The specifications of the vehicles are listed in Table 2 on page 8. A model is developed for each individual vehicle to estimate the fuel consumption at a given vehicle speed and road condition as described below.

The vehicle longitudinal dynamics at the speed of v and road angle θ_{r} with a vehicle mass of M_{v}, rolling resistance C_{r}, and vehicle frontal area A_{v} is described by

$$M_{\mathrm{v}}\dot{v} = \frac{T_{\mathrm{e}} r_{\mathrm{g}} r_{\mathrm{d}} \eta_{\mathrm{d}}}{r_{\mathrm{w}}} - C_{\mathrm{d}} \rho A_{\mathrm{v}} v^2 - M_{\mathrm{v}} g (C_{\mathrm{r}} cos\theta_{\mathrm{r}} + sin\theta_{\mathrm{r}}), \tag{8}$$

where T_{e} is the engine torque, r_{g} and r_{d} are the gear and differential ratios, r_{w} is the wheel radius, η_{d} is the driveline efficiency, ρ is the air viscosity, g is the gravitational acceleration, and C_{d} is the drag coefficient. In this work, reductions in C_{d} due to platooning are ignored. Even though this may cause an underestimation of vehicle accelerations and MPG, this modeling error is not relevant due to the model-free and data-driven nature of the optimization framework. In real applications, the platooning effects on C_{d} will be embedded in the speed and MPG measurements. The diesel engine torque is estimated using the injected fuel rate $\dot{m}_{\mathrm{f}}$, compression ratio r_{c}, the heat specific ratio γ, and the engine torque losses due to friction T_{f} and pumping T_{p} as presented by Hand et al. (2013) using

$$T_{\mathrm{e}} = \xi \left(\dot{m}_{\mathrm{f}} \Big(1 - \frac{1}{r_c^{\gamma-1}} \Big) \right) - T_{\mathrm{p}} - T_{\mathrm{f}}, \tag{9}$$

where ξ is represents the combustion efficiency (Hand et al., 2013). The engine friction loss is calculated from a polynomial correlation with the engine speed N_{e},

$$T_{\mathrm{f}} = \frac{V_{\mathrm{d}}}{4\pi}(c_0 + c_1 N_{\mathrm{e}} + c_2 N_{\mathrm{e}}^2), \tag{10}$$

with V_{d} as the engine cylinder volume and c_1, c_2 and c_3 as the model parameters. At a specific gear level (GL), the engine speed N_{e} is calculated based on the vehicle speed from (8) assuming the torque converter is in locked position. The vehicle gear shifting logic is designed to calculate GL at time step k based on the previous gear level, the engine speed N_{e} and the commanded pedal angle θ_{ped} using

$$\mathrm{GL}(k) = f_{\mathrm{gl}}(N_{\mathrm{e}}, \theta_{\mathrm{ped}}, \mathrm{GL}(k-1)), \tag{11}$$

where f_{gl} represents the shift logic designed for acceptable driveability and such that the engine operates always between the speed lines shown in Figure 4. The maximum and minimum engine speed (ω) for each line shown in Figure 4 are a function of GL(k), as listed in Table 2. The pumping loss T_{p} is calculated based on the exhaust (P_{em}) and intake (P_{im}) manifold pressure difference at each operating condition

$$T_p = \frac{V_d}{4\pi}(P_{\mathrm{em}} - P_{\mathrm{im}}). \tag{12}$$

The manifold pressures in (12) are calculated from the engine filling dynamics. Details of the engine model and tuning its parameters can be found in (Hand et al., 2013; Salehi, Stefanopoulou, Kihas, & Uchanski, 2016).

The desired injected fuel $\dot{m}_{\mathrm{f}}$ in this work is calculated by the vehicle cruise controller such that the vehicle tracks the desired speed V_{set}.

$$\dot{m}_{\mathrm{f},i}(s) = \left(\frac{K_I}{s} + K_p \right) \left(V_{\mathrm{i,set}}(s) - V_{\mathrm{i}}(s) \right), \; i = \{\mathrm{lead}, \mathrm{follow}\} \tag{13}$$

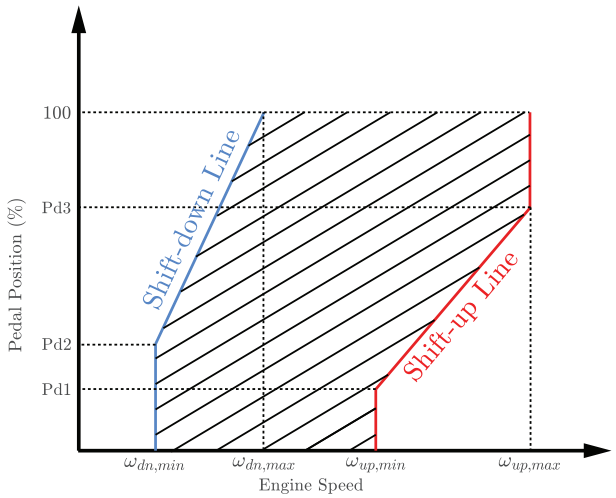

Figure 4.: Illustration of the designed gear shift strategy. The gear shift (up or down) happens when the engine operating point goes out of the hatched area.

Table 2.: Specifications of the lead and follow vehicles

	Heavy Duty Vehicle	**Medium Duty Vehicle**
Engine Family	Detroit Diesel DD13	Ford Powerstroke
Vehicle Mass (kg)	36287	10112
Gearbox	6 speed	6 speed
Vehicle frontal area, $A_{\mathrm{v}}(\mathrm{m}^2)$	10	3.58
Drag Coefficient, $C_{\mathrm{d}}(-)$	0.7	0.36
Rolling Coefficient $C_{\mathrm{r}}(-)$	0.008	0.0034
$[Pd_1, Pd_2, Pd_3]$ %	[0,0,100]	[0.15,0.45,0.8]
$\omega_{\mathrm{dn,min}}$ (rpm)	800	750
$\omega_{\mathrm{dn,max}}$ (rpm)	[1150,1150,1150,1150,1100,1050]	1600
$\omega_{\mathrm{up,min}}$ (rpm)	[1800,1350,1300,1250,1200,1200]	1400
$\omega_{\mathrm{up,max}}$ (rpm)	[1900,1800,1750,1600,1500,1500]	[2600,2800,2800,2900,3000,3100]

Finally, one can calculate the vehicle fuel economy MPG $= v/\dot{m}_{\mathrm{f}}$ from (8) - (13).

Figure 5 shows the results of the fuel economy and gear level at different vehicle speeds for both the lead and following vehicles assuming $\theta_{\mathrm{r}} = 0$ when both acceleration from $v_0 =$ 10 mph and deceleration from $v_0 = 70$ mph are simulated. The vehicle fuel economy varies discontinuously at the instants of gear shift as shown in Figure 5a. Also a hysteresis is observed in the fuel economy curve that reflects the hysteresis in the gear shift logic, which is applied commonly in automatic shift logics to improve driveability and avoid chattering at the speed of gear change.

4. Simulation Results

Optimization results on a flat terrain including the utility function J, vehicle speed, and fuel economy are shown in Figure 6 for two different test scenarios with different initial speeds using the parameter values listed in Table 1. As Figure 6 shows, it takes about 10 steps for the optimization algorithm to calculate the optimal speed of 44 mph for both cases of initial speed ($v_{\mathrm{p},0} = 20$ mph and $v_{\mathrm{p},0} = 60$ mph). These 10 steps are taken in approximately 1500 seconds due to the requirement that data from the vehicles are collected only after the platoon fuel consumption reaches a steady state condition (i.e. $v_{\mathrm{L}} \approx v_{\mathrm{F}} \approx v_{\mathrm{p}}$ and $\Delta\dot{m}_{\mathrm{f}} \approx 0$) every time a new speed setpoint is issued and the lead vehicle's large payload increases the settling time. The steady state condition was realized by adding a conservative waiting time to a data collector in simulations after each change in the speed setpoint. This convergence time is considered

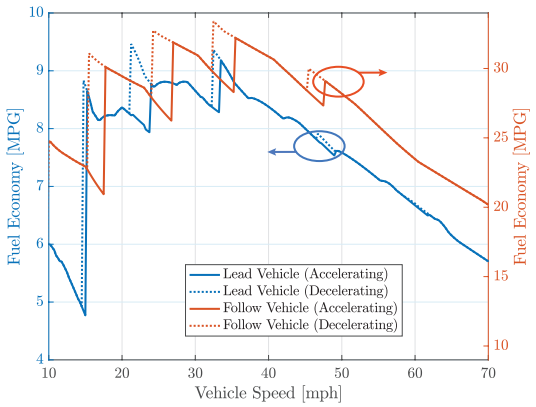

(a) Fuel economy calculated for both vehicles in acceleration and deceleration test (simulation results).

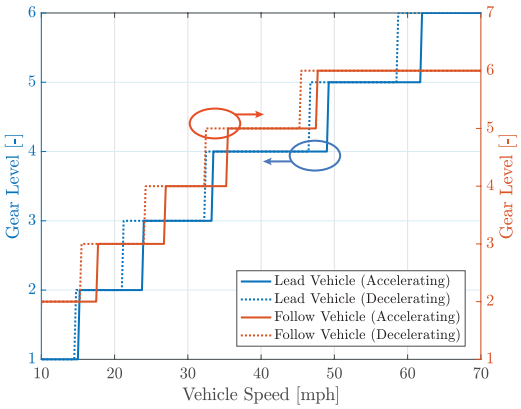

(b) Gear level comparison between two vehicles. The shifting speed depends on the vehicles' acceleration.

Figure 5.: Fuel economy and gear level comparison between the lead and follow vehicles. The ovals with the arrows indicate the corresponding y-axes.

acceptable for the purposes of this work and even for long-haul missions, but could be improved by minimizing the wait time through a smart detection of when steady state has been reached. Furthermore, for a platoon with lighter vehicles with shorter settling times, the convergence time is expected to be shorter.

A small overshoot/undershoot is observed for the platoon reference speed v_{p} in each test scenario. This small overshoot is a result of the particular selection of the parameters used in this case study. This set of parameters is preferred, because the minor aggressiveness that causes the overshoot is also observed to help avoid local optima as discussed in detail in Section 5.

Simulation test results are summarized in Figure 7. Compared with initial speed $v_{\mathrm{p},0} = 20$ mph and desired cruising speed $v_{\mathrm{p,des}} = 60$ mph, the optimized speed $v_{\mathrm{p}} = 44$ mph has 19.3% and 4.9% utility improvement, respectively. The utility improvement over the initial speed is achieved through 40.0% more mobility with 2.2% less fuel economy, whereas the utility improvement over the desired speed is due to 18.4% more fuel economy at the cost of 7.5% mobility. Hence, the proposed method is capable of achieving a balance between fuel economy and mobility. Due to the existence of gear shift hysteresis, the utility and fuel economy of the platoon is different in acceleration and deceleration cases as discussed in Section 4 and 5. However, Figure 7 shows that the optimization algorithm has successfully approached the maximum point in the utility curve at the speed of 44 mph for both initial speeds considered. The discontinuity and hysteresis observed in Figure 7 leads to the discussion about dependency of the final speed on the Nelder-Mead parameters in the following section.

A second simulation is performed for a varying road grade condition. In particular, optimization results including the utility function J, vehicle speed, and fuel economy are shown in Figure 8 for a scenario with a step increase in road grade and using the same parameter values as the flat terrain case. The road grade increases from 0% to 1.5% at $t = 3000$ s and it is assumed that the on-board sensors are able to detect this change to reinitialize the algorithm. Note that only the information that there is a change in the road grade is needed to trigger the reinitialization, and not the actual grade value. A fuel economy drop is observed in the figure after $t = 3000$ s. The optimal cruising speeds found by the algorithm for the two different road grades are demonstrated and compared with their corresponding utility functions in Figure 9. The model-free algorithm is able to achieve the new optimal operating point after the road grade changes. Because the fuel economy is significantly reduced after the grade change, the algorithm correctly exploits this opportunity to increase mobility instead to maximize utility.

Finally, to provide a sense for the sensitivity of the results to the utility function weights, Figure 10 shows the results for the flat road scenario under various weights α_{M} while keeping α_{F} constant. As the relative weight on mobility increases, the optimal speed approaches the

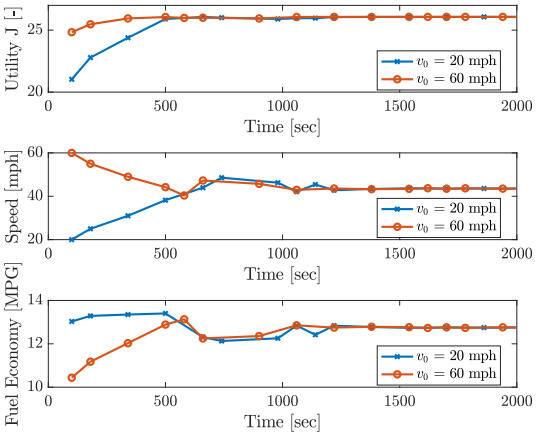

Figure 6.: Simulation results from testing the proposed platoon speed management for different initial speeds.

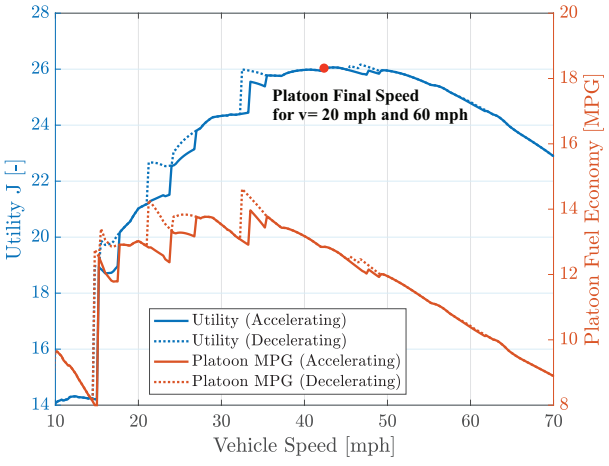

Figure 7.: MPG and utility functions of the platoon during acceleration from 10 mph and deceleration from 70 mph. The final speeds obtained with the platoon speed management from the initial speeds of 20 mph and 60 mph are shown with red dots that overlap.

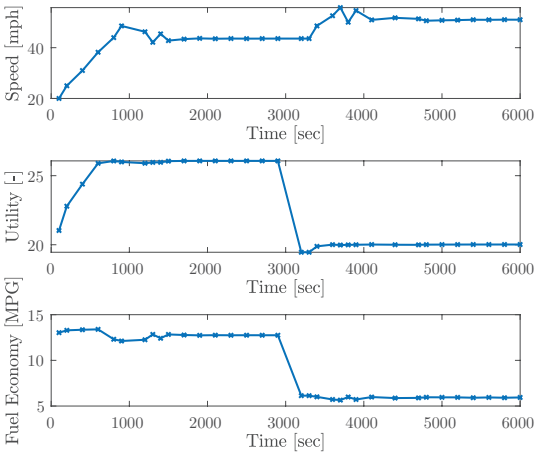

Figure 8.: Simulation results from testing the proposed platoon speed management with a step increase in road grade.

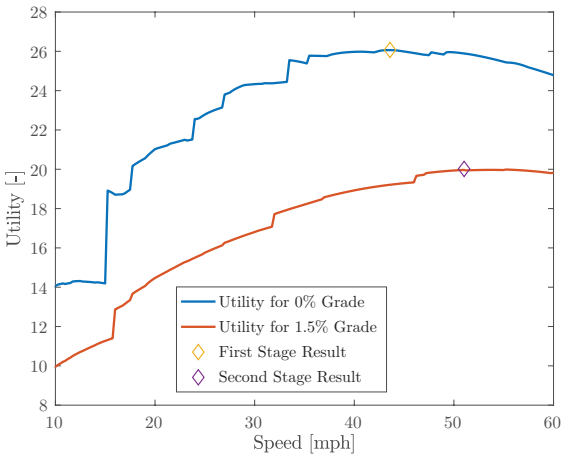

Figure 9.: Utility functions and the optimal points found by the algorithm in the varying road grade case.

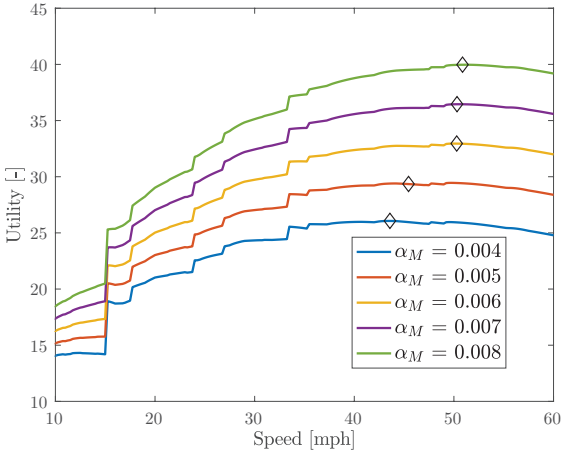

Figure 10.: Sensitivity analysis for α_{M}. The diamonds represent the optimization results from the algorithm.

desired speed and the algorithm is able to find the optimal solution in each case.

5. Sensitivity Analysis of the Nelder-Mead Parameters

In this section, the impacts of various parameters of Nelder-Mead on the performance of the algorithm are discussed. These parameters control the performance of the four Nelder-Mead optimization steps, namely, reflection, expansion, contraction and shrink as shown in Figure 2. Hence, this section serves as a guideline for designing the Nelder-Mead algorithm in model-free platoon speed management.

Figure 11 shows the impact of the expansion parameter γ on the speed and corresponding utility when the initial speed is 20 mph. As the expansion parameter γ increases, the algorithm adopts a more aggressive behavior, typically leading to a shorter rise time in speed, but also a higher overshoot. Here, rise time is the time at which the speed has reached 90% of the final speed value. On the other hand, the settling time, defined as the time at which the speed enters and remains within 2% of the final value, varies without a clear trend as summarized in Figure 12. With a γ as low as 1.2, the overshoot in speed reduces as Figure 11 shows, but the chance of being trapped in a local optimum also increases. Similar to the expansion parameter γ, increasing the reflection parameter Γ increases overshoot, but reduces the rise time, which is also illustrated in Figure 12.

On the other hand, the effect of the contraction parameter ρ on the final results is not significant for the ranges considered. This is because the contraction process does not occur frequently in this case. The same conclusion also applies to the shrink parameter σ; those results are omitted for brevity.

In summary, the suggested parameter intervals for this problem are as follows: 0.7-1.2 for the reflection parameter Γ, 1.5-2 for the expansion parameter γ, 0.25-0.75 for the contraction parameter ρ, and 0.25-0.75 for the shrink parameter σ. Within these ranges, the parameters can be tuned as explained above to adjust the trade-off between avoiding overshoots, achieving faster convergence, and increasing the chance of avoiding local optima.

6. Experimental Validation

Experimental validation is performed using two engine test cells with diesel engines representative of the two vehicle types considered in this study. Specifically, one test cell is equipped with

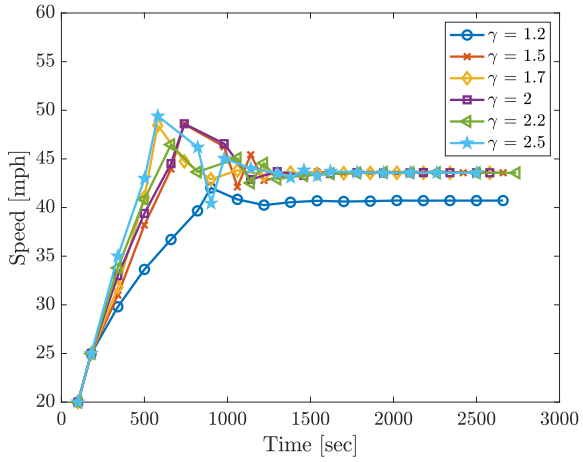

Figure 11.: Platoon speed vs. time when the initial speed is 20 mph for different expansion values.

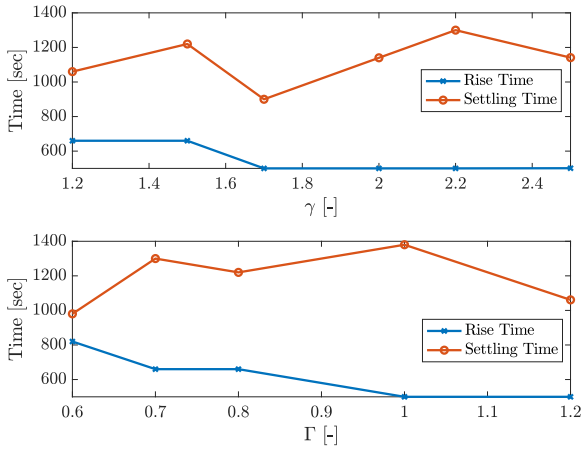

Figure 12.: Sensitivity of the Nelder-Mead rise and settling times to the parameters γ and Γ. The rise time decreases while no clear trend is observed for increasing γ and Γ.

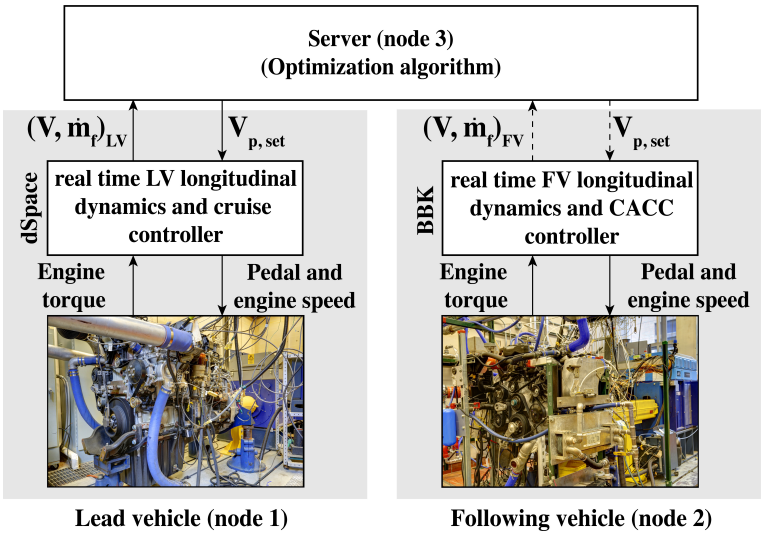

Figure 13.: Illustration of the connected testbed system. Solid lines indicate cable connections, whereas dashed lines represent connections over the Internet.

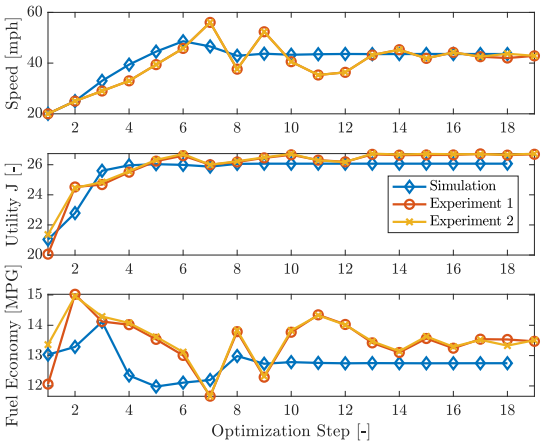

Figure 14.: Simulation vs. experimental data: Exp 1 and Exp 2, $v_0 = 20$ mph, $\gamma = 2$

an inline 6-cylinder 12.8L diesel engine for a heavy duty truck (the lead vehicle, LV), whereas the other one is equipped with a V8 6.7L diesel engine corresponding to a medium duty truck (the following vehicle, FV). Both test cells have engine-in-the-loop simulation capability, i.e., the engines can run in closed-loop with vehicle models running in real time (Kim et al., 2014). To emulate the connectivity between the vehicles in the platoon, the networked hardware-in-the-loop simulation paradigm is leveraged (Ersal et al., 2011; Ersal, Brudnak, Stein, & Fathy, 2012; Ersal, Gillespie, Brudnak, Stein, & Fathy, 2013).

In particular, the two test cells are connected over the Internet to emulate a network of two connected vehicles as illustrated in Figure 13. In this setup, the first node comprises the heavy-duty engine coupled with a dSPACE system simulating the heavy-duty lead vehicle model. The coupling between the engine and the dSPACE system is such that the dSPACE system commands the pedal and engine speed and receives the engine torque measurements from the engine. Furthermore, the dSPACE system communicates with the server PC (node 3), receives the platoon speed setpoints and returns the actual speed and the instantaneous fuel rate of the heavy-duty vehicle. The second node has a similar architecture as the first node, except that a PC with a BBK-PCI card is used instead of a dSPACE system to simulate the medium-duty following vehicle dynamics in real time in closed-loop with the medium-duty engine. Node 2 sends the medium-duty vehicle's speed and instantaneous fuel rate to the server over the Internet and receives the platoon speed setpoint. Similar to the simulation case, the recording and exchange of data is executed after the platoon reaches the desired steady-state speed. The information exchange over the Internet is done using the User Datagram Protocol (UDP). The Quality of Service (QoS) of the network used in this work is high to the extent that the packet delays are negligible and there are no packet drops.

Four engine-in-the-loop experiments are performed from the same initial platoon speed of $v_0 = 20$ mph; two experiments with the expansion parameter $\gamma = 2$ for validation purposes (Experiments 1 and 2), and two experiments with $\gamma = 1.5$ to demonstrate the implications of a poorly tuned algorithm (Experiment 3 and 4).

Figure 14 shows the comparison between the experimental results and the simulation results for Experiment 1 and 2. The utility trends between the simulation results and experimental results are similar, albeit the absolute values are different, which is expected due to errors in modeling the engines in the simulation study. Note that this good agreement in the performance of the algorithm between the simulation and experimental results is achieved without any re-tuning when transitioning from simulations to experiments. Moreover, the iteration trajectories are consistent between the two experiments, demonstrating good repeatability despite the noise that can be observed in the fuel economy measurements shown in the third plot of Figure 14. Hence, the results highlight the robustness benefits of the proposed formulation.

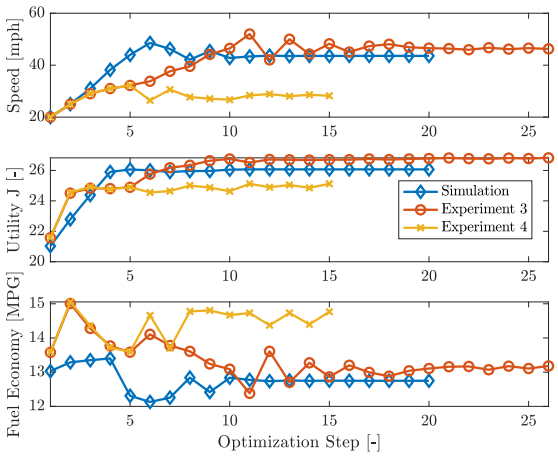

Figure 15.: Simulation vs. experimental data: Exp 3 and Exp 4, $v_0 = 20$ mph, $\gamma = 1.5$. An inappropriate Nelder-Mead parameter set leads to local optimum.

On the other hand, Figure 15 illustrates the results when a poorly tuned Nelder-Mead with $\gamma = 1.5$ is chosen for Experiment 3 and 4. In this case, not only there is a larger difference between the simulation and experimental results, but also the repeatability of the experimental results is lower. In particular, in the Experiment 4, the algorithm chooses a path significantly different from the other three experiments. This is caused by the increased sensitivity of the algorithm to the noise in data collection due to a poor choice of γ. Specifically, during the data acquisition process, even after the system reaches the steady state, the fuel economy measurement varies due to noise as pointed out previously. As shown in Figure 16, this affects the utility values of Step 3 and Step 5 for both Experiment 3 and Experiment 4 even when their speed values are the same. The utility value of Step 3 is less than the utility value of Step 5 in Experiment 3, while the utility value of Step 3 is greater than the utility value of Step 5 in Experiment 4, which leads to an expansion step in Experiment 3 in contrast to a contraction step that happens in Experiment 4. The relatively conservative setting of the expansion parameter as the one used in Experiment 4 renders the algorithm more sensitive to noise, which leads to a local optimum. As shown in Step 5 of the optimization for the Experiment 4, the algorithm decides to decelerate rather than the continuous acceleration observed in Experiment 1, 2 and 3. The algorithm is thus finally trapped into a local maximum caused by the gear shift nonlinearity.

The convergence to local maximum is not observed with the larger expansion coefficient of $\gamma = 2$. As discussed in Section 5, with increased γ, the search space expands with relatively more aggressive overshoots and undershoots. However, the chance to converge to a global optimum increases. With small γ, a moderate search speed is obtained, giving rise to increased chance to be trapped in a local maximum. Hence, for practical reasons, a larger value of expansion parameter γ is appreciated at the cost of larger overshoot.

The experimental results in Figure 16 show that the algorithm converges in about 20 steps at most when the optimization setting is aggressive, compared to the 10 steps observed for simulations in Figure 7. These 20 steps are taken in around 2100 seconds. This long convergence time is because the algorithm needs to wait between the iterations for the platoon to settle to the new steady state and a conservative wait time was adopted in the experiments to ensure testbed safety. Furthermore, the convergence speed in terms of time reported here is significantly influenced by the very slow dynamics of the lead vehicle due to its very large mass. Convergence speeds are expected to reduce with minimized wait times to proceed to the next speed setpoint after steady state has been reached and in platoons of lighter vehicles. Nevertheless, increasing the convergence speed is identified as an important future research direction.

Finally, the model-free algorithm successfully manages to increase the utility in all cases, including the Experiments 3 and 4 despite the challenges described above due to a relatively

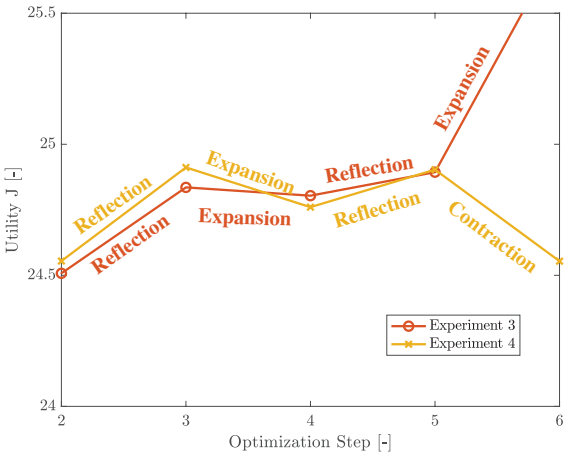

Figure 16.: Exp 3 and Exp 4, Step 2 to Step 5, $v_0 = 20$ mph, $\gamma = 1.5$. In Exp 4, the utility at Step 5 is smaller than utility at Step 3 despite a speed increasing, thus a contraction happens in contrast to Exp 3 where an expansion happens at Step 6.

poor choice of γ.

7. Conclusion

A model-free framework for managing the speed of a platoon to adjust the balance between fuel economy and mobility as characterized by travel speed is presented. The framework relies on an optimization formulation with a linear combination of the fuel economy and mobility metrics. This optimization problem is solved using the Nelder-Mead approach in a data-driven, model-free manner. A case study is performed both in simulation and using networked engine-in-the-loop experiments on an example platoon of two vehicles, and both the simulation and experimental results confirm the advantages and disadvantages of the developed method.

In particular, the algorithm is found effective in increasing utility (i.e., the objective function) without the need for any vehicle or powertrain model. However, due to its data-driven nature and the need to collect these data in steady-state, it requires to wait until the end of the transient period after each iteration to perform the data collection, which can prolong its convergence in terms of time, especially for the heavy duty vehicle with very large payload considered in the presented case study. Although the algorithm improves utility continuously and one does not need to wait until it converges to reap its benefits, the convergence time may be too long in certain applications, e.g., if continuous disturbances prevent the platoon from reaching steady state for extended periods of time. Even though the convergence times are expected to be smaller for lighter vehicles, improving the convergence time is identified as an important future research direction.

Funding

This work was supported by the Automotive Research Center (ARC) in accordance with Cooperative Agreement W56HZV-14-2-0001 U.S. Army Combat Capabilities Development Command (CCDC) Ground Vehicle System Center (GVSC) Warren, MI. DISTRIBUTION STATEMENT A. Approved for public release; distribution unlimited.

This material is based upon work supported by the National Science Foundation under Grant No. 1646019.

References

Alam, A., Mårtensson, J., & Johansson, K. H. (2013). Look-ahead cruise control for heavy duty vehicle platooning. In *IEEE Conference on Intelligent Transportation Systems* (p. 928-935).

Aliotta, J. (2017). *Driving the army's energy-efficient future.* `https://www.army.mil/article/181692/driving_the_armys_energy_efficient_future`. ([Online; accessed 22-April-2019])

Bergenhem, C., Pettersson, H., Coelingh, E., Englund, C., Shladover, S., & Tsugawa, S. (2012). Overview of platooning systems. In *Intelligent Transport Systems World Congress* (p. EU-00336).

Caltagirone, L., Torabi, S., & Wahde, M. (2015). Truck platooning based on lead vehicle speed profile optimization and artificial physics. In *IEEE Conference on Intelligent Transportation Systems* (pp. 394–399).

Chan, E. (2012). Overview of the SARTRE platooning project: Technology leadership brief. *SAE Technical Papers*, *2012-01-9019*.

Chang, K. S., Hedrick, J. K., Zhang, W.-B., Varaiya, P., Tomizuka, M., & Shladover, S. E. (1993). Automated highway system experiments in the path program. *Journal of Intelligent Transportation Systems*, *1*(1), 63-87.

Deutschle, S., Kessler, G. C., Lank, C., Hoffmann, G., Hakenberg, M., & Brummer, M. (2010). Use of electronically linked Konvoi truck platoons on motorways. *AutoTechnology*, *10*(4), 20–25.

Englund, C., Chen, L., Ploeg, J., Semsar-Kazerooni, E., Voronov, A., Bengtsson, H. H., & Didoff, J. (2016). The grand cooperative driving challenge 2016: boosting the introduction of cooperative automated vehicles. *IEEE Wireless Communications*, *23*(4), 146-152.

Ersal, T., Brudnak, M., Salvi, A., Stein, J. L., Filipi, Z., & Fathy, H. K. (2011). Development and model-based transparency analysis of an internet-distributed hardware-in-the-loop simulation platform. *Mechatronics*, *21*(1), 22-29.

Ersal, T., Brudnak, M., Stein, J. L., & Fathy, H. K. (2012). Statistical transparency analysis in internet-distributed hardware-in-the-loop simulation. *IEEE/ASME Transactions on Mechatronics*, *17*(2), 228-238.

Ersal, T., Gillespie, R. B., Brudnak, M., Stein, J. L., & Fathy, H. K. (2013). Effect of coupling point selection on distortion in internet-distributed hardware-in-the-loop simulation. *International Journal of Vehicle Design*, *61*(1-4), 67-85.

Hand, M. J., Hellström, E., Kim, D., Stefanopoulou, A., Kollien, J., & Savonen, C. (2013). Model and calibration of a diesel engine air path with an asymmetric twin scroll turbine. In *ASME Internal Combustion Engine Division Fall Technical Conference* (pp. V001T05A010–V001T05A010).

Hargreaves, S. (2011). *Ambushes prompt military to cut energy use.* `http://money.cnn.com/2011/06/14/news/economy/military_energy_strategy/index.htm`. ([Online; accessed 22-April-2019])

Hoffenson, S., Arepally, S., & Papalambros, P. Y. (2014). A multi-objective optimization framework for assessing military ground vehicle design for safety. *The Journal of Defense Modeling and Simulation*, *11*(1), 33-46.

Kim, Y., Salvi, A., Siegel, J. B., Filipi, Z., Stefanopoulou, A., & Ersal, T. (2014). Hardware-in-the-loop validation of a power management strategy for hybrid powertrains. *Control Engineering Practice*, *29*(Special Issue: ECOSM12), 277-286.

Li, S. E., Li, R., Wang, J., Hu, X., Cheng, B., & Li, K. (2016). Stabilizing periodic control of automated vehicle platoon with minimized fuel consumption. *IEEE Transactions on Transportation Electrification*, *3*(1), 259–271.

Liang, K.-Y., Mårtensson, J., & Johansson, K. H. (2016). Heavy-duty vehicle platoon formation for fuel efficiency. *IEEE Transactions on Intelligent Transportation Systems*, *17*(4), 1051–1061.

Liu, H., Shladover, S. E., Lu, X.-Y., & Kan, X. D. (2020). Freeway vehicle fuel efficiency improvement via cooperative adaptive cruise control. *Journal of Intelligent Transportation Systems*, 1-13.

Milanés, V., & Shladover, S. E. (2016). Handling cut-in vehicles in strings of cooperative adaptive cruise control vehicles. *Journal of Intelligent Transportation Systems*, *20*(2), 178-191.

National Highway Traffic Safety Administration. (2006). *CAFE overview.* `https://web.archive.org/web/20061205030159/http://www.nhtsa.dot.gov/cars/rules/cafe/overview.htm`. ([Online; accessed 22-April-2019])

Nelder, J. A., & Mead, R. (1965). A simplex method for function minimization. *The Computer Journal*, *7*(4), 308-313.

Nemeth, B., Csikos, A., Varga, I., & Gaspar, P. (2012). Road inclinations and emissions in platoon control via multi-criteria optimization. In *Mediterranean Conference on Control and Automation* (pp. 1524–1529).

Ploeg, J., Scheepers, B. T. M., van Nunen, E., van de Wouw, N., & Nijmeijer, H. (2011). Design and experimental evaluation of cooperative adaptive cruise control. In *IEEE Conference on Intelligent Transportation Systems* (p. 260-265).

Rajamani, R., Tan, H. S., Law, B. K., & Zhang, W. B. (2000). Demonstration of integrated longitudinal and lateral control for the operation of automated vehicles in platoons. *IEEE Transactions on Control Systems Technology*, *8*(4), 695–708.

Salehi, R., Stefanopoulou, A. G., Kihas, D., & Uchanski, M. (2016). Selection and tuning of a reduced parameter set for a turbocharged diesel engine model. In *American Control Conference* (p. 5087-5092).

Tsugawa, S., & Kato, S. (2010). Energy ITS: Another application of vehicular communications. *IEEE Communications Magazine*, *48*(11), 120–126.

Tsugawa, S., Kato, S., & Aoki, K. (2011). An Automated Truck Platoon for Energy Saving. *IEEE/RSJ International Conference on Intelligent Robots and Systems*, 4109–4114.

Turri, V., Besselink, B., & Johansson, K. H. (2016). Gear management for fuel-efficient heavy-duty vehicle platooning. In *IEEE Conference on Decision and Control* (pp. 1687–1694).

Turri, V., Besselink, B., & Johansson, K. H. (2017). Cooperative look-ahead control for fuel-efficient and safe heavy-duty vehicle platooning. *IEEE Transactions on Control Systems Technology*, *25*(1), 12-28.

U.S. Department of Energy. (2019). *Platooning trucks to cut cost and improve efficiency.* `https://www.energy.gov/eere/articles/platooning-trucks-cut-cost-and-improve-efficiency`. ([Online; accessed 22-April-2019])

Varaiya, P. (1993). Smart Cars on Smart Roads: Problems of Control. *IEEE Transactions on Automatic Control*, *38*(2), 195–207.

Wang, C., & Nijmeijer, H. (2015). String stable heterogeneous vehicle platoon using cooperative adaptive cruise control. In *IEEE Conference on Intelligent Transportation Systems* (p. 1977-1982).

Wang, Z., Wu, G., & Barth, M. J. (2018). A review on cooperative adaptive cruise control (CACC) systems: Architectures, controls, and applications. In *IEEE Conference on Intelligent Transportation Systems* (p. 2884-2891).

Wang, Z., Wu, G., Hao, P., Boriboonsomsin, K., & Barth, M. (2017). Developing a platoon-wide eco-cooperative adaptive cruise control (CACC) system. In *IEEE Intelligent Vehicles Symposium* (p. 1256-1261).

Zabat, M., Stabile, N., Farascaroli, S., & Browand, F. (1995). The aerodynamic performance of platoons: A final report. *California Partners for Advanced Transit and Highways (PATH)*, *UCB-ITS-PRR-95-35*.

Zheng, Y., Bian, Y., Li, S., & Li, S. E. (2019). Cooperative control of heterogeneous connected vehicles with directed acyclic interactions. *IEEE Intelligent Transportation Systems Magazine*.